01 Apr 1991

Some Stability and Control Aspects of a Variable Pivot Wing Configuration

Paul Vitt

SOME STABILITY AND CONTROL ASPECTS OF A VARIABLE PIVOT WING CONFIGURATION

Paul Vitt

Abstract

In supersonic flight, there is a large positive shift in the static margin, which causes extreme positive shifts in longitudinal stability, and is an undesirable characteristic. This paper investigates some of the stability and control aspects of an alternative configuration, that of a variable pivot wing aircraft -- an aircraft with two sets of wings, one set sweeps forward, the other set sweeps rearward. By prescribing a sweep schedule, it is desired to minimize the static margin shift with Mach number. The effects of the two lift elements -- that of mechanical shift of the center of pressure forward with sweep, and aerodynamic coupling with the reduction in aspect ratio which cause a decrease in lift-curve slope due to sweep -- on simple longitudinal stability and control parameters will be presented. Two cases are examined. The first case has four equal-area wings with a fuselage/strake; the second case has the area of the front wings twice the area of the rearward wings with a fuselage\strake.

Nomenclature

b	wing span
c	wing chord
C_{La}	lift-curve slope
$C_{La}(\Phi_f/\Phi_r)$	lift-curve slope for (wing sweep angles)
C_{ma}	moment-curve slope
$C_{ma}(\Phi_f/\Phi_r)$	moment-curve slope for (wing sweep angles)
M	Mach number
MAC	mean aerodynamic chord
S	wing area
ST	stagger (in chord lengths)
XMC	moment center location
/R	aspect ratio
Φ	wing sweep angle

Subscripts

f	forward wing pair
r	rear (or aft) wing pair

Introduction

The major trade-off of high speed flight is the conflicting requirements of high aspect ratio wings for high lift and maneuverability at low speeds with low aspect ratio wings for low gust loading and wave drag at supersonic speeds. Variable configurations were proposed to solve this problem, by varying the aspect ratio of the wings to fit the current flight regime. The two current designs are for aft-sweeping wings and oblique-sweeping wings. Both have their drawbacks: sweeping the wings aft causes a mechanical shift in center of pressure which augments the shift normally associated with supersonic flight; the oblique-swept wing causes obvious longitudinal-lateral-directional stability and control cross-coupling, which leads to undesirable handling qualities. A newer alternative is the scissor wing (ref [2]), which has four wings cross-joined (forward-to-aft) across a single center pivot. This paper does an initial investigation of some of the characteristics of a derivative of this concept, the variable pivot wing configuration. It also has four wings, but are set in pairs (two wings sweep forward

synchronously, and similarly two wings sweep rearward), and each wing has an individual pivot, which is close to the aircraft centerline. This gives the advantage of being able to have longitudinally unsymmetrical sweep scheduling: sweeping the forward wings faster than the aft wings, for example. The wings can be fully extended for low speed flight, in order to give good handling capabilities, and then can be swept to any combination of angles to minimize the shift in static margin, wave drag and gust loadings at high speeds. Cross-coupling of longitudinal and lateral-directional attributes is eliminated due to the centerline symmetry of the aircraft.

The preliminary investigation presented here deals with simple stability and control derivatives, specifically the lift-curve slope, the moment-curve slope, and the static margin. For this purpose, two variations of the variable pivot wing were examined: the first model has four equal-area wings, a strake or fuselage, and a horizontal tail; the second model has the total wing area split 2:1 between the forward reference wings and the aft reference wings, a fuselage or strake, and a horizontal tail.

The objective of this paper is to show that the static margin shift can be controlled for a large range of Mach numbers by prescribing a sweep schedule which takes advantage of the variable forward/aft sweep capabilities of the design. Also, the mechanisms which produce the resulting lift-curve slopes and moment-curve slopes will be examined, in order to determine how the control is achieved. High speed flight has many factors which are not considered here, and knowledge of the mechanics which control longitudinal stability will allow the designer to trade-off the stability and control with performance efficiently.

Method of Analysis

The linear vortex lattice method of reference [5] (NARUVLE) was used as a subroutine in a program to iteratively trim the aircraft, using the horizontal tail for a given flight condition, to determine the aerodynamic characteristics. Transonic results cannot be obtained with this method because it is linear. The method was limited to 200 panels, and in some cases gave some numerical oscillation. Reference [3] indicates that the trends obtained can be taken as accurate.

In order to study the effects of variable sweep on static margin, three models were developed and analyzed over a Mach number range of 0.4 to 3.4. All configuration used the same /R and reference wing area (S), so that the results could be related (the /R and S for the pivot wing configurations was taken from a basic sweep of Φ = 18 degrees). The first is the baseline, which is a conventional, fixed wing aircraft based roughly on a F-18 layout, and is used to give the results a basis for comparison. This configuration is shown in Figure 1a. The second is the equal-area configuration, which has four paired equal-area wings. This is the basic variable pivot wing layout, and it is shown in Figures 1b, 1c, and 1d, for various sweep angles. In order to study the effects of wing area and aspect ratio on the static margin, a split-area configuration was developed. For the split-area configuration, there are four paired wings, but the forward pair have twice the area of the aft pair (or the total wing area is split 66%/33%). The equal-area and split-area models are shown in Figures 2a and 2b, respectively, in the basic sweep positions. The pivots for the wings are located 1.733 ft off of the centerline of the aircraft to allow for the necessary mechanisms for rotation of the wing, and also to allow the front section of the wings to fold into the fuselage without overlapping each other. The geometry of the different configurations is listed in Table 1. The total aircraft weight was taken to be 50,000 lbs, with the equal area wing weights 4000 lbs each, and the split-area wing weights 5333 lbs forward and 2667 lbs aft.

Table 1. Configuration Geometries

Parameter	Baseline	Equal-Area	Split-Area
S (ft^2)	426.0	427.9	424.5
b (ft^2)	39.33	41.35[c]	41.35[c]
		39.33[d]	39.33[d]
c_{root} (ft)	16.00	6.84	9.00[a]
			4.44[b]
c_{tip} (ft)	5.33	3.30	4.50[a]
			2.22[b]
MAX (ft)	11.09	5.18[2]	6.81[a,2]
			3.45[b,2]
Taper Ratio	0.33	0.48	0.5
/R[1]	3.63	4.00[c]	4.03[c]
		3.62[d]	3.64[d]
		2.00[e]	2.01[e]
		1.00[f]	1.01[f]
/R[2]	3.63	7.24	5.39[a]
			11.22[b]
$S_{H.\ Tail}$ (ft^2)	98.72	98.72	98.72
XMC (ft)	32.67	30.32	29.57

NOTES: 1 - total configuration
2 - individual wings
a - forward wing pair
b - aft wing pair
c - $\Phi = 0°$
d - $\Phi = 18°$
e - $\Phi = 45°$
f - $\Phi = 60°$

Each of the variable-pivot models was evaluated for symmetrical ($\Phi_f = \Phi_r$) sweep cases of Φ = 0, 18, 30, 45, and 60 degrees, and the unsymmetrical sweep cases which were permutations of Φ = 30, 45, and 60 degrees. The unsymmetrical sweep cases will be denoted by ($\Phi_f = \Phi_r$).

Aerodynamic coupling between the wings has been linked to the stagger of the wings: the horizontal distance between the front and aft wings. The results of reference [6], which are used to interpret the results obtained here, are for two dimensional airfoils, so the stagger is measured from the leading edge of MAC_r, to the trailing edge of the MAC_f. The stagger for the equal-area models ranged from 1.64MAC for the no sweep case to 3.72MAC for the fully swept case. The split-area models had a similar range, based on an average MAC_a = 5.13 ft., of 1.62MAC_a to 3.71MAC_a for the unswept and fully swept cases, respectively. Reference [6] indicates that strong coupling (increasing the front wing lift and decreasing the rear wing lift significantly) occurs for stagger less than 3 and moderate coupling occurs for stagger between 3 and 10. This is the reason for XMC to be as far forward as it is relative to the wing locations.

All three models were designed with a 5% stable static margin (the pivot wing configurations were 5% stable with sweep Φ = 18°) at M = 0.4. The shift in XMC with unsymmetrical sweep is taken into account by using the wing weights listed above.

Results and Discussion

Equal-area Wing-Strake Model

The lift-curve results are shown in Figures 3a and 3b. The (0/0) case showed an increased lift-curve slope at subsonic and low supersonic speeds over the baseline case, and the curves all tended to follow the same trend of slowly decreasing as M increases. The lowest sweep (highest /R and closely coupled aerodynamically) wing pair dominates the C_{La} response of the model. From Figure 3a, if the response of the low sweep configurations (0/0) and (30/30) is taken to be the trend, the (45/45) and (60/60) sweep settings require increased Mach number to converge to that trend. Figure 3b shows the effects of sweeping the alternate pair to an unsymmetric position. Sweeping the alternate to a lower sweep forces the response to the trend to converge at lower Mach number. The (30/60) and (45/30) follow the (30/30) trend very closely -- although the (30/60) case is shifted slightly down due a reduction in total wing lifting area. The (45/60) case closely follows the (45/45) case. These results indicate that the lift-curve slope is very dependent on the magnitude of the largest /R and the stagger of the wings, both factors are linked together by sweep. The (60/60) case decreases very little with increasing Mach number.

The moment-curve results are shown in Figure 4. A large unstable moment-curve slope results at low supersonic speeds for two cases: a low front sweep/high rear sweep or for both wings highly swept. The first result is due to the much higher $C_{La}$of the front wing forcing a positive couple. The second result is most likely due to a shift in the total center of pressure forward (after reference [4]), due to coupling (ST = 3.72) increasing the lift of the front wing (relative to the aft wing) and the mechanical forward sweep of the wing.

The combination of these results into the static margin is shown in Figure 5. The results are strongly influenced by any large changes in either C_{La} or C_{ma}. The $\Phi = 45°$ case exhibited a sharp increase in stability for $1.2 < M < 1.8$, and a similar pattern is followed by the (30/60) case. For this Mach number range, C_{La}(45/45) is nearly constant, so the increase in stability is due to the shift of the center of the pressure of the wings aft from increasing Mach number, reducing the forward wing moment arm about XMC, reducing C_{ma}. The (30/60) case stability increase is due to a reduction in C_{La} as well as the pressure shift. The least shift in static margin at higher Mach numbers occur for the (60/60) case, which is due to the almost constant lift-curve slope and the slowly changing moment-curve slope. The sweep schedule for the least shift in static margin is shown in Figure 6. The wings are initially swept to (45/30) by M = 1.45, and then to (60/60) by M = 1.8, keeping the static margin constant at 5% stable up to this point, and then increasing along the (60/60) curve. This result will be discussed later.

Split-Area Wing-Strake Model

The lift-curve slope results for the split-area wing-strake model are shown in Figure 7. The $\Phi = 0°$ case showed a large improvement in C_{La} over the wing-strake baseline case in both the subsonic and low supersonic regimes. The interesting result from this graph is the effect of forward wing sweep on the lift-curve slope, when the aft wing is fully swept. Comparing the (30/60), (45/60), and (60/60) cases shows that the sweep of the front wing controls C_{La}. As the front wings are swept forward the stagger is increased and the lifting ability of the rear wing is increased as the lifting ability and area of the front wing is decreased. So, because of the area distribution, the model's lifting ability is decreased. With both sets of wings fully swept, the lift-curve slope becomes virtually independent of Mach number.

The moment-curve slope results are shown in Figure 8. None of the curves shows a large negative gain (below the trend line) like the other models have. By sweeping the front wing

from (30/60) to (45/60) reduces the negative shift of the curve for low supersonic Mach numbers. As the forward wings are swept, the stagger is increased, which decreases the relative lifting ability of the front wing, while increasing the relative lifting ability of the rear wing. The aspect ratio of the front wing is also reduced, which further decreases C_{L_a}. Both of these effects induce a negative moment about XMC. The positive moment that is the result must then be because of the mechanical shift of the forward wing's aerodynamic center.

The static margin results are presented in Figure 9. The main result is that in order to control the static margin the aft wing needs to be fully swept at supersonic speeds, in order to minimize its /R and coupling effects and so reduce the impact it has on stability. Then the front wing can use its large lifting area to control the static margin. The sweep schedule for this case is shown in Figure 6. The relation between the front wing and the rear wing characteristics is shown here. The front wing is swept from 30 to 60 and then down to 45° as Mach number increases from 1.2 to 1.85, while the aft wing is swept to 60° before M = 1.35. The reason for the front wing gyrations is at low speeds and when the rear wing is at 45°, low stagger is required to maintain stability, hence the Φ_f = 30°. When the rear wing is initially swept to 60°, the forward wing must be fully swept in order to increase the stagger and reduce the effectiveness of the front wing to maintain stability. Then, as Mach number increases, the center of pressure shifts aft on the front wing and its sweep must be reduced to increase its effectiveness through an increased /R and aerodynamic coupling, and force the center of pressure to stay forward.

Comparison of the Scheduled Static Margins

The results of the applying the sweep schedules to the different wing-strake models are shown in Figure 10. The pivot wing models showed less static margin increase than the baseline model did. The pivot-wing configurations showed considerable improvement over the baseline models at the low end of the supersonic range (for M < 2.0), with the variable pivot wings able to maintain their 5% static margin to Mach = 1.8. The baseline model did not maintain the 5% margin above the subsonic range. The split-area model had the least center of pressure travel of all three models, with the increased front lifting surface being able to exert more control as

the center of pressure shifts aft. The equal-area wing-strake model did not have the same degree of control at higher supersonic Mach numbers.

Conclusions

A preliminary evaluation of the ability of a variable pivot wing aircraft to control the lift-curve and moment-curve slopes, and hence static margin, was presented. In comparison to a conventional highspeed aircraft layout, the variable pivot wing showed exceptional control over the static margin shift in the supersonic regime.

It was shown that the wing-strake models were able to maintain a 5% static margin up to Mach numbers of approximately 1.8, and the static margin rise after this point was minimal. The control of the static margin is a complicated function of the interaction between the aspect ratios of the wing pairs, the aerodynamic coupling between the wings, mechanical shifts in the aerodynamic centers of the wings, and reduction in wing area due to masking by the fuselage (or the symmetrical wing in the pair in the wing-only cases). The aerodynamic coupling and aspect ratio effects are linked through sweep: this study did not attempt to separate the effects, but incorporated them together into the results, as on an actual model they would be linked.

The effects of low- and high-speed control and other stability derivatives, and wave drag needs to be evaluated on the models, because these aspects were not considered in this paper. These factors will probably compromise the benefits of this design in some ways -- for example, limiting the forward sweep to be within the nose shock. They should be investigated, since the design showed considerable improvement over the baseline conventional configuration in terms of control of stability at high speeds.

References

1. Housch, C. S. "Aerodynamic Characteristics of Scissor Wing Geometries". Master's Thesis, University of Missouri-Rolla, 1990.

2. Rokhsaz, K. "Scissor Wing, Patent Disclosure". Disclosure #87-UMR-023, 1986.

3. Rokhsaz, K., and Selberg, B. "Scissor Wing -- An Alternative to Variable Sweep". 27th Aerospace Sciences Meeting, AIAA, 1989.

4. Selberg, B., Rokhsaz, K., and Housch, C. "Some Aerodynamic Characteristics of the Scissor Wing Configuration." SAE paper #892202, Aerospace Tech. Conf. and Exposition, 1989.

5. Tulinius, J. "Unified Subsonic, Transonic, and Supersonic NAR Vortex Lattice" North American Rockwell, TFD72-523, 1972.

6. Keith, M. W. and Selberg, B. P. "Aerodynamic Canard/Wing Parametric Analysis for General-Aviation Applications." J. Aircraft, Vol. 22, No. 5, May 1985, pp 401-485.

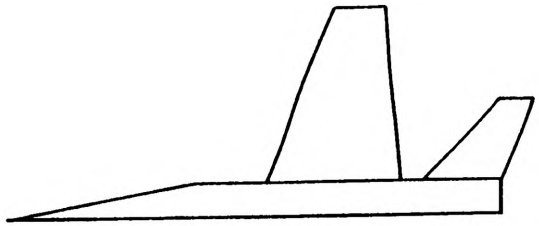

Figure 1a: Wing-strake baseline configuration

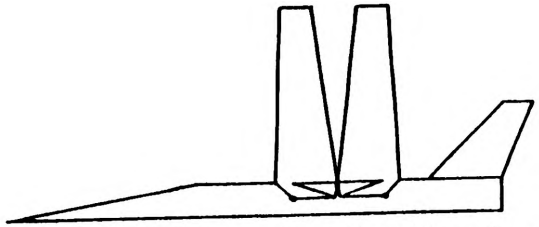

Figure 1b: Variable pivot configuration, Φ = 0°

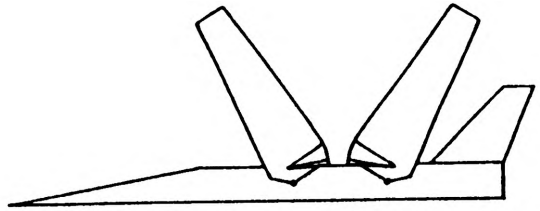

Figure 1c: Variable pivot configuration, Φ = 30°

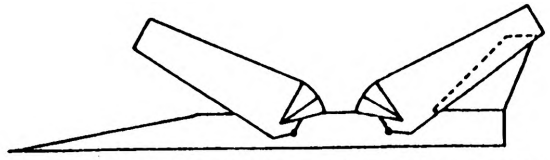

Figure 1d: Variable pivot configuration, Φ = 60°

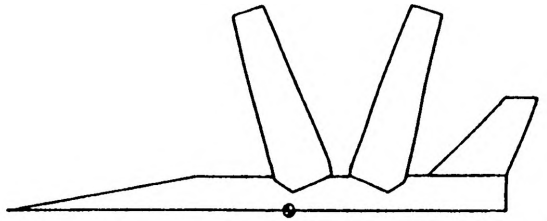

Figure 2a: Equal-area wing-strake model (Φ = 18°)

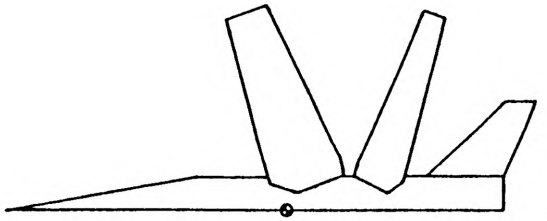

Figure 2b: Split-area wing-strake model (Φ = 18°)

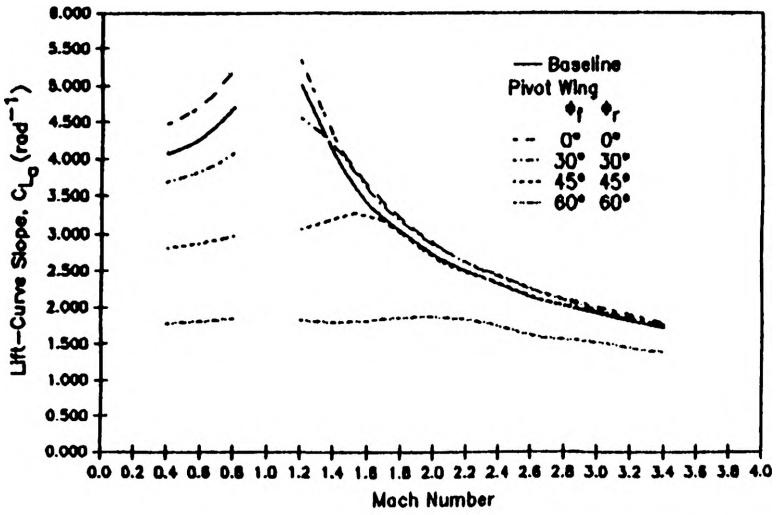

Figure 3a: Lift-curve slopes for the equal-area wing-strake model

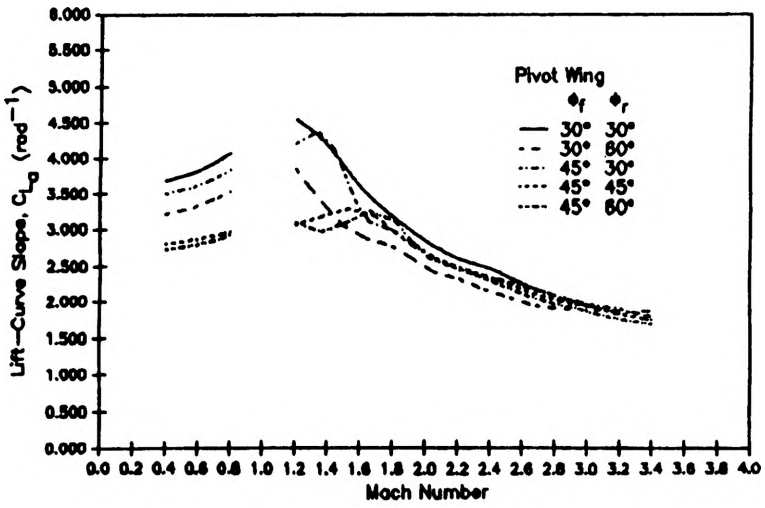

Figure 3b: Lift–curve slopes for the equal–area wing–strake model (continued)

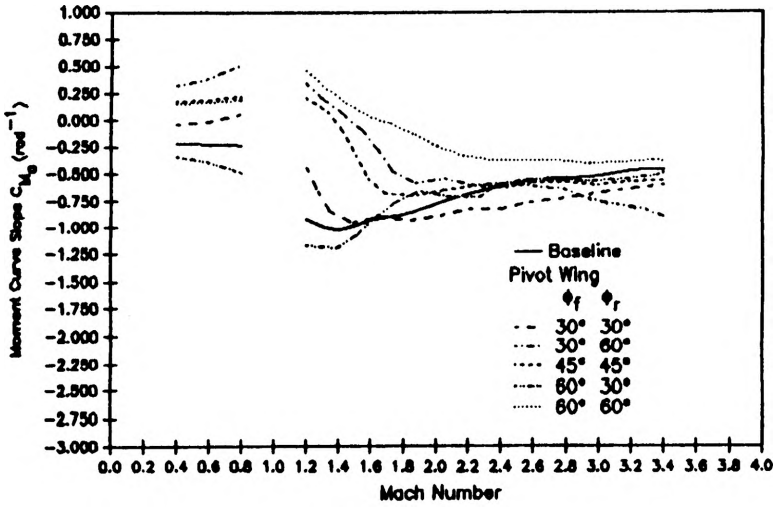

Figure 4: Moment–curve slopes for the equal–area wing–strake model

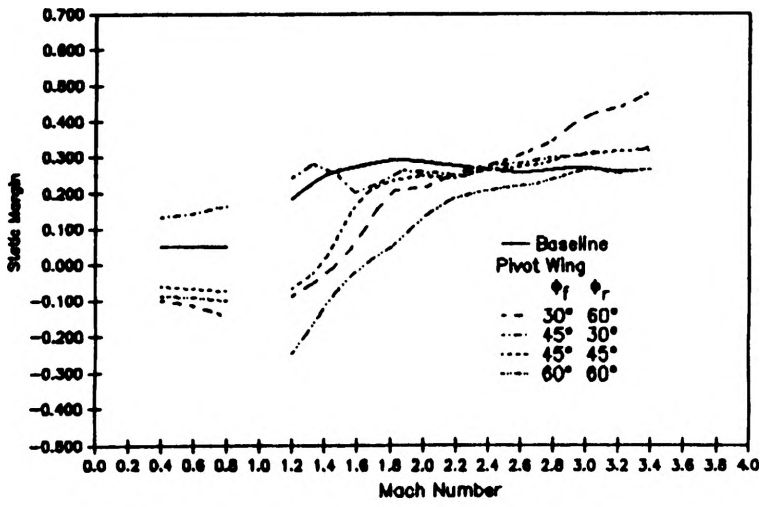

Figure 5: Static margin plots for the equal–area wing strake model

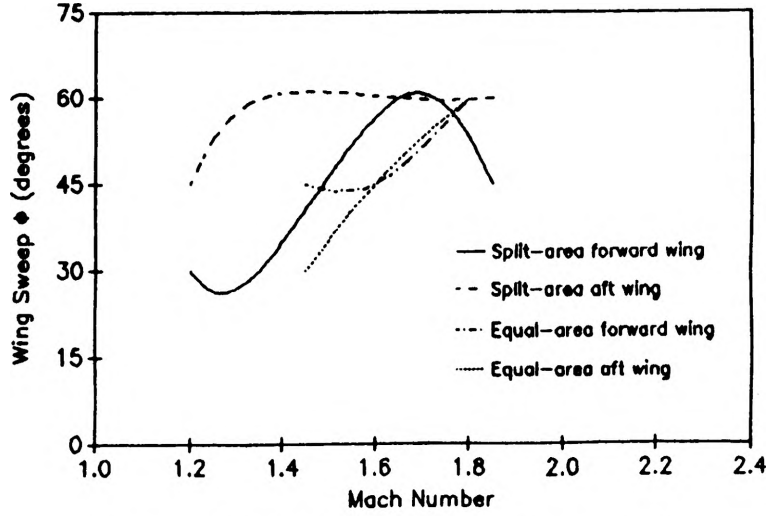

Figure 6: Sweep Schedule for the split–area and equal–area wing–strake models

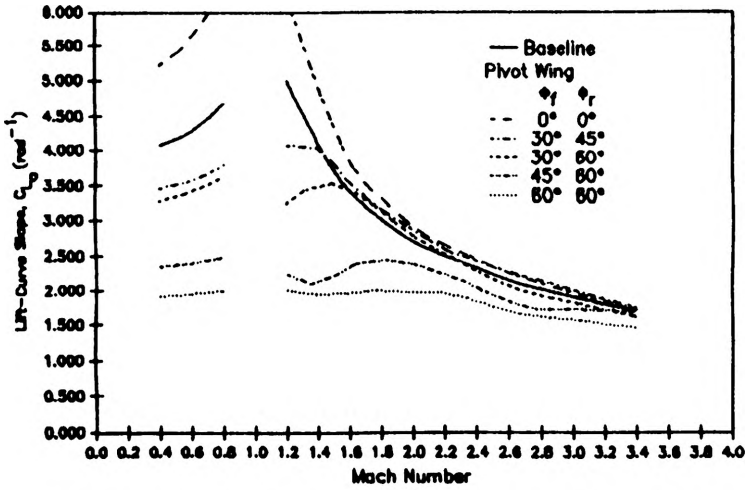

Figure 7: Lift-curve slopes for the split-area wing-strake model

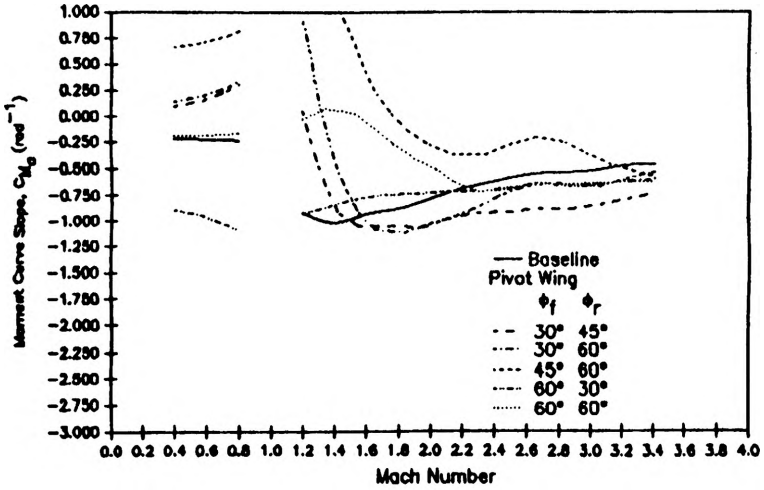

Figure 8: Moment-curve slopes for the split-area wing-strake model

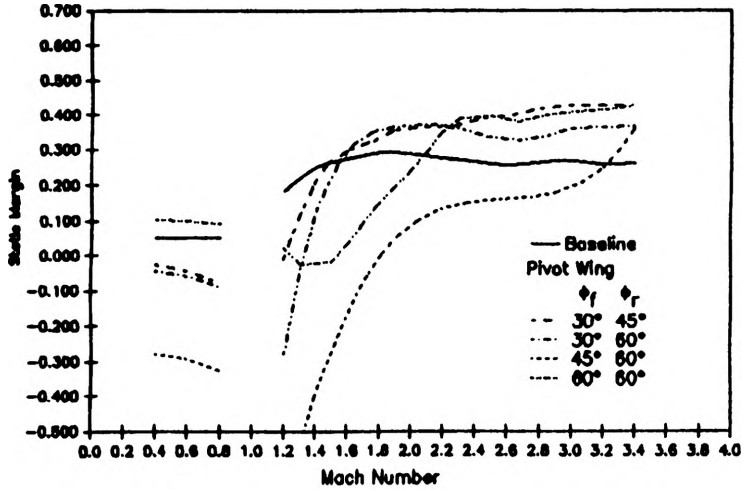

Figure 9: Static margin plots for the split-area wing-strake model

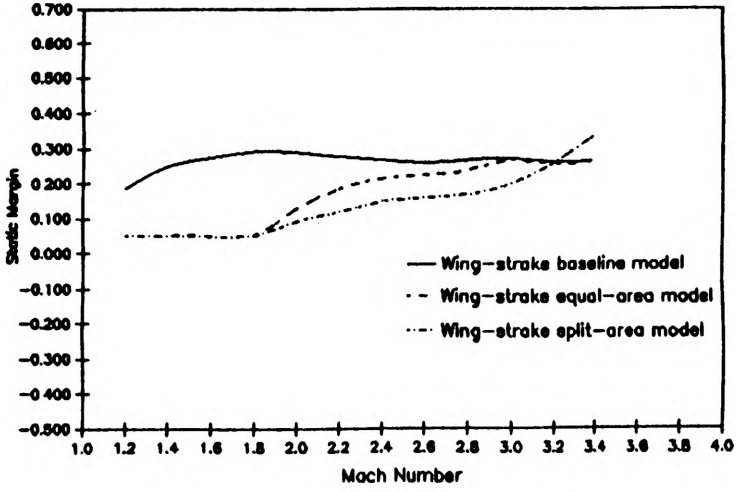

Figure 10: Static margin control comparison for the different models using the sweep schedules